

Addressing Limitations in Existing ‘Simplified’ Liquefaction Triggering Evaluation Procedures: Application to Induced Seismicity in the Groningen Gas Field

R.A. Green¹, J.J. Bommer², A. Rodriguez-Marek³, B.W. Maurer⁴,
P.J. Stafford⁵, B. Edwards⁶, P.P. Kruiver⁷, G. de Lange⁸, and J. van Elk⁹

Abstract The Groningen gas field is one of the largest in the world and has produced over 2000 billion m³ of natural gas since the start of production in 1963. The first earthquakes linked to gas production in the Groningen field occurred in 1991, with the largest event to date being a local magnitude (M_L) 3.6. As a result, the field operator is leading an effort to quantify the seismic hazard and risk resulting from the gas production operations, including the assessment of liquefaction hazard. However, due to the unique characteristics of both the seismic hazard and the geological subsurface, particularly the unconsolidated sediments, direct application of existing liquefaction evaluation procedures is deemed inappropriate in Groningen. Specifically, the depth-stress reduction factor (r_d) and the Magnitude Scaling Factor (MSF) relationships inherent to existing variants of the simplified liquefaction evaluation procedure are considered unsuitable for use. Accordingly, efforts have first focused on developing a framework for evaluating the liquefaction potential of the region for moment magnitudes (M) ranging from 3.5 to 7.0. The limitations of existing liquefaction procedures for use in Groningen and the path being followed to overcome these shortcomings are presented in detail herein.

Keywords Liquefaction, liquefaction hazard, magnitude scaling factor, depth-stress reduction factor, induced seismicity, Groningen gas field

¹Professor, Dept. of Civil and Environmental Engineering, Virginia Tech, Blacksburg, VA, USA (email: rugreen@vt.edu)

²Senior Research Investigator, Department of Civil and Environmental Engineering, Imperial College London, London, UK

³Professor, Dept. of Civil and Environmental Engineering, Virginia Tech, Blacksburg, VA, USA

⁴Assistant Professor, Dept. of Civil and Environmental Engineering, University of Washington, Seattle, WA, USA

⁵Reader, Dept. of Civil and Environmental Engineering, Imperial College London, London, UK

⁶Senior Lecturer, School of Environmental Sciences, University of Liverpool, Liverpool, UK

⁷Senior Geophysicist, Deltares, Delft, the Netherlands

⁸Senior Engineering Geologist, Deltares, Delft, the Netherlands

⁹Development Lead Groningen Asset, Nederlandse Aardolie Maatschappij B.V., Assen, the Netherlands

1 Introduction

The Groningen gas field is located in the northeastern region of the Netherlands and is one of the largest in the world. It has produced over 2000 billion m³ of natural gas since the start of production in 1963. The first earthquakes linked to gas production in the Groningen field occurred in 1991, although earthquakes were linked to production at other gas fields in the region since 1986. To date the largest induced earthquake due to production at the Groningen field is the 2012 local magnitude (M_L) 3.6 Huizinge event, and the largest recorded peak ground acceleration (PGA) is 0.11 g which was recorded during a more recent, smaller (M_L 3.4) event. In response to concerns about the induced earthquakes, the field operator Nederlandse Aardolie Maatschappij (NAM) is leading an effort to quantify the seismic hazard and risk resulting from the gas production operations (van Elk et al. 2017). In view of the widespread deposits of saturated sands in the region, the risk due to earthquake-induced liquefaction is being evaluated as part of this effort. Although an almost negligible contributor to earthquake fatalities, liquefaction triggering is an important threat to the built environment and in particular to infrastructure and lifelines (e.g., Bird and Bommer 2004).

Central to the liquefaction hazard/risk assessment of the Groningen field is the stress-based “simplified” liquefaction evaluation procedure, which is the most widely used approach to evaluate liquefaction potential worldwide. While most of the recently proposed variants of this procedure yield similar results for scenarios that are well represented in the liquefaction case history databases (e.g., Green et al. 2014), their predictions deviate, sometimes significantly, for other scenarios (e.g., small and large magnitude events; very shallow and very deep liquefiable layers; high fines content soils; medium dense to dense soils). These deviations result partly because existing variants of the simplified procedure are semi-empirical, hence they are apt for replicating existing data but lack proper extrapolation power. The empirical elements of existing procedures are derived from data from tectonic earthquakes in active shallow-crustal tectonic regimes such as California, Japan, and New Zealand. These conditions are different from those in the Groningen field. Moreover, the geologic profiles/soil deposits in Groningen differ significantly from those used to develop the empirical aspects of the simplified procedure. As a result, the suitability of

existing variants of the simplified procedure for direct use to evaluate liquefaction in Groningen is questionable. Accordingly, prior to assessing the liquefaction hazard in Groningen, efforts have first focused on developing a framework for performing the assessment. This actually required a step backwards to develop an “unbiased” liquefaction triggering procedure for tectonic earthquakes, due to biases in relationships inherent to existing variants of the simplified procedure (e.g., Boulanger and Idriss 2014).

In the following sections, the shortcomings in current variants of the simplified procedures for use in Groningen are detailed. Then, the efforts to develop a new “unbiased” variant of the simplified liquefaction evaluation procedure are presented. An outline of how this procedure is being modified for use in Groningen is presented next, followed by a brief overview of how the liquefaction hazard of Groningen will be assessed.

2 Shortcoming in existing variants of the simplified liquefaction evaluation procedure for use in Groningen

2.1 Overview of the simplified procedure

As mentioned in the Introduction, the stress-based simplified liquefaction evaluation procedure is central to the approach adopted to assess the liquefaction hazard in the Groningen region. The word “simplified” in the procedure’s title originated from the proposed use of a form of Newton’s Second Law to compute cyclic shear stress (τ_c) imposed at a given depth in the soil profile, in lieu of performing numerical site response analyses (Whitman 1971; Seed and Idriss 1971). Inherent to this approach for computing the seismic demand is an empirical depth-stress reduction factor (r_d) that accounts for the non-rigid response of the soil profile and a Magnitude Scaling Factor (MSF) that accounts for the effects of the shaking duration on liquefaction triggering. For historical reasons the duration of a moment magnitude (**M**) 7.5 earthquake is used as the reference for MSF.

Case histories compiled from post-earthquake investigations were categorized as either “liquefaction” or “no liquefaction” based on whether evidence of liquefaction was or was not observed. The seismic demand (or normalized Cyclic Stress Ratio: CSR*) for each of the case

histories is plotted as a function of the corresponding normalized/fines-content corrected *in situ* test metric, e.g., Standard Penetration Test (SPT): $N_{1,60cs}$; Cone Penetration Test (CPT): q_{c1Ncs} ; or small strain shear-wave velocity (V_s): V_{s1} . In this plot, the “liquefaction” and “no liquefaction” cases tend to lie in two different regions of the graph. The “boundary” separating these two sets of case histories is referred to as the Cyclic Resistance Ratio ($CRR_{M7.5}$) and represents the capacity of the soil to resist liquefaction during an **M** 7.5 event for level ground conditions and an effective overburden stress of 1 atm. This boundary can be expressed as a function of the normalized *in situ* test metrics.

Consistent with the conventional definition for factor of safety (FS), the FS against liquefaction (FS_{liq}) is defined as the capacity of the soil to resist liquefaction divided by the seismic demand:

$$FS_{liq} = \frac{CRR_{M7.5}}{CSR^*} \quad (1)$$

The Dutch National Annex to the Eurocode for the seismic actions (i.e., NPR 9998 2017), recommends the use of the Idriss and Boulanger (2008) variant of the simplified liquefaction evaluation procedure, but allows other variants to be used if they are in line with the safety philosophy of the NPR 9998-2017. As a result, the Idriss and Boulanger (2008) variant and the updated variant (Boulanger and Idriss 2014) have been used in several liquefaction studies in Groningen, resulting in predictions of potentially catastrophic liquefaction effects that have severe implications for buildings and for infrastructure such as dikes.

2.2 Depth-stress reduction factor: r_d

As stated above, r_d is an empirical factor that accounts for the non-rigid response of the soil profile. Both the Idriss and Boulanger (2008) and Boulanger and Idriss (2014) variants of the simplified liquefaction evaluation procedure use an r_d relationship that was developed by Idriss (1999). As shown in Figure 1, the Idriss (1999) r_d relationship is a function of earthquake magnitude and depth, with r_d being closer to one for larger magnitude events (note that $r_d = 1$ for all depths corresponds to the rigid response of the profile). This is because larger magnitude events have longer characteristic periods and, hence, ground motions with longer wavelengths. As a result,

even a soft profile will tend to respond as a rigid body if the characteristic wavelength of the ground motions is significantly longer than the overall thickness of the profile. Accordingly, the correlation between earthquake magnitude and the frequency content of the earthquake motions significantly influences the r_d relationship. This raises questions regarding the appropriateness of the Idriss (1999) relationship, which was developed using motions recorded during tectonic events, for evaluating liquefaction potential in Groningen where the seismic hazard is dominated by induced earthquakes having magnitudes less than M 5.

Another issue with the Idriss (1999) r_d relationship is that it tends to predict overly high CSR^* values at depth in a soil profile for tectonic events. This bias is illustrated in Figure 1 and is pronounced for depths between ~ 3 to 20 m below the ground surface. As a result, when used to evaluate case histories to develop the $CRR_{M7.5}$ curves that are central to the procedure, the biased r_d relationship results in a biased positioning of the $CRR_{M7.5}$ curve. The significance of this issue is mitigated to some extent when the same r_d relationship used to develop the $CRR_{M7.5}$ curve is also used in forward analyses (i.e., the bias cancels out). However, this will not be the case if site/region-specific r_d relationships are developed and used in conjunction with a $CRR_{M7.5}$ curve that was developed using a “biased” r_d relationship.

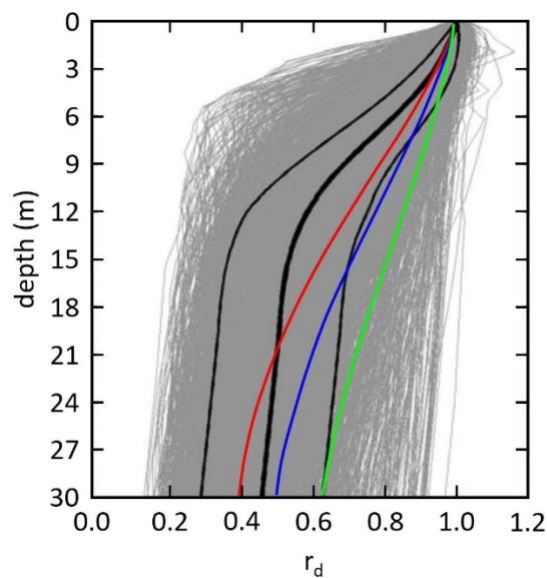


Fig. 1 The red, blue, and green lines were computed using the Idriss (1999) r_d relationship for M 5.5, M 6.5, and M 7.5 events, respectively. The grey lines were computed by Cetin (2000) from

equivalent linear site response analyses performed using a matrix of 50 soil profiles and 40 motions. The black lines are the median (thick line) and median plus/minus one standard deviation (thinner lines) for the Cetin (2000) analyses.

2.3 Magnitude Scaling Factor: MSF

As stated above, MSFs account for the influence of the strong motion duration on liquefaction triggering. MSFs have traditionally been computed as the ratio of the number of equivalent cycles for an $M 7.5$ event to that of a magnitude M event, raised to the power b [i.e., $MSF = (n_{eqM7.5}/n_{eqM})^b$]. Both the Idriss and Boulanger (2008) and Boulanger and Idriss (2014) procedures used the Seed et al. (1975) variant of the Palmgren-Miner (P-M) fatigue theory to compute $n_{eqM7.5}$ and n_{eqM} from earthquake motions recorded at the surface of soil profiles. Furthermore, they obtained the value of b from laboratory test data. The parameter b is the negative of the slope of a plot of $\log(CSR)$ versus $\log(N_{liq})$, as shown in Figure 2; N_{liq} is the number of cycles required to trigger liquefaction in a soil specimen subjected to sinusoidal loading having an amplitude of CSR, typically determined using cyclic triaxial or cyclic simple shear tests.

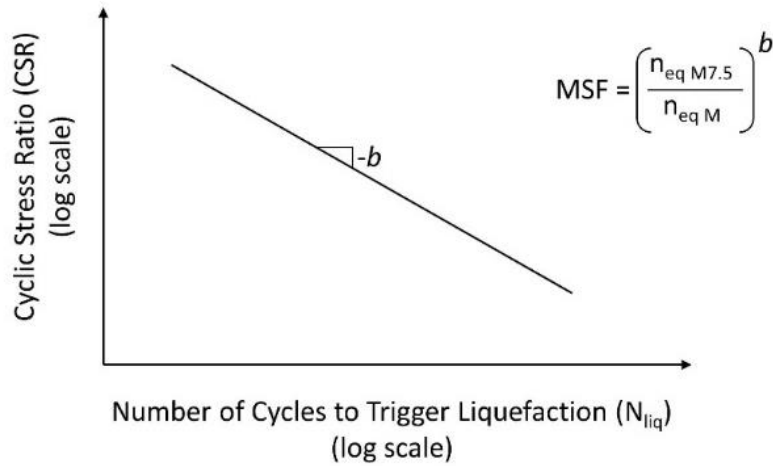


Fig. 2 Relationship between laboratory CSR vs. N_{liq} and MSF.

There are several shortcomings inherent to the approach used by Idriss and Boulanger (2008) and Boulanger and Idriss (2014) to compute the number of equivalent cycles (n_{eq}) and MSF. These include:

- Both the magnitude and uncertainty of n_{eq} , and hence MSF, are assumed to be constant with depth. However, Green and Terri (2005) have shown that n_{eq} can vary with depth in a given profile and Lasley et al. (2017) showed that while the median value for n_{eq} computed for a large number of soil profiles and ground motions is relatively constant with depth, the uncertainty in n_{eq} varies with depth.
- Pulses in the acceleration time history having an amplitude less than $0.3 \cdot a_{max}$ are assumed not to contribute to the triggering of liquefaction, and thus are not considered in the computation of n_{eq} . Using a relative amplitude criterion to exclude pulses is contrary to the known nonlinear response of soil which is governed by the absolute amplitude of the imposed load, among other factors. The use of a relative amplitude exclusion criterion with tectonic earthquake motions may inherently bias the resulting MSF.
- Each of the two horizontal components of ground motion is treated separately, inherently assuming that both components have similar characteristics. However, analysis of recorded motions has shown this is not always the case, particularly in the near fault region (e.g., Green et al. 2008; Carter et al. 2016). Groningen ground-motions recorded at short source-to-site distances often display pronounced polarization (Stafford et al. 2018).
- The b values used by Boulanger and Idriss (2014) were derived from several laboratory studies performed on various soils and it is uncertain whether all these studies used a consistent definition of liquefaction in interpreting the test data. As a result, the b values proposed by Boulanger and Idriss (2014) entail considerable uncertainty (Ulmer et al. 2018), with the proposed values not being in accord with those inherent to the shear modulus and damping degradation curves used in the equivalent linear site response analyses to develop the r_d correlations (a point elaborated upon subsequently).
- Recent studies have shown that the residuals of the amplitude and duration of earthquake ground motions are negatively correlated (e.g., Bradley 2011) and this feature is clearly observed in the Groningen data (Bommer et al. 2016). None of the MSF correlations developed to date, to include the one proposed by Boulanger and Idriss (2014), have considered this.

Some of the shortcomings listed above will be more significant to the Groningen liquefaction hazard assessment than others, but it is difficult to state *a priori* which ones these are. Furthermore, even for tectonic earthquakes the validation of MSF relationships is hindered by the limited

magnitude range of case histories in the field liquefaction databases, with the majority of the cases being for events having magnitudes ranging from **M** 6.25 to **M** 7.75 (NRC 2016). Specific to the Groningen liquefaction hazard assessment, MSFs for small magnitude events are very important, particularly given that published MSF relationships vary by a factor of 3 for **M** 5.5 (Youd et al. 2001), with this factor increasing if the proposed MSF relations are extrapolated to smaller magnitudes.

3 Removing bias from the simplified liquefaction evaluation procedure for tectonic earthquakes

3.1 Depth-stress reduction factor: r_d

A new relationship for r_d was developed by Lasley et al. (2016) using an approach similar to that used by Cetin (2000). Equivalent linear site response analyses were performed on 50 soil profiles compiled by Cetin (2000) that are representative of those in the liquefaction case history databases. However, Lasley et al. (2016) used a larger set of recorded input motions in their analyses than were available at the time of the Cetin (2000) study. Although Cetin (2000) and Lasley et al. (2016) used different software to perform their site response analyses, both codes employed the equivalent linear algorithm to model the soil response. Whereas several studies have shown that different nonlinear site response codes can give very different results, equivalent linear site response codes tend to be consistent in terms of their output (e.g., Lasley et al. 2014).

Several functional forms for r_d were examined by Lasley et al. (2016) in regressing the results from the site response analyses, with the following form selected because of its simplicity and fit of the data (i.e., relatively low standard deviation of the regressed data):

$$r_d = (1 - \alpha) \exp\left(\frac{-z}{\beta}\right) + \alpha + \varepsilon_{r_d} \quad (2a)$$

where z is depth in meters, α is the limiting value of r_d at large depths and can range from 0 to 1, the variable β controls the curvature of the function at shallow depths, and ε_{r_d} is a zero-mean,

normally distributed random variable with standard deviation σ_{r_d} . Expressions for α and β are:

$$\alpha = \exp(-4.373 + 0.4491 \cdot M) \quad (2b)$$

$$\beta = -20.11 + 6.247 \cdot M \quad (2c)$$

and σ_{r_d} is defined as:

$$\sigma_{r_d} = \frac{0.1506}{[1 + \exp(-0.4975 \cdot z)]} \quad (2d)$$

Relative to the other r_d relationships inherent to commonly used variants of the simplified procedure, the Lasley et al. (2016) model was developed using more site response data and more rigorous regression analyses. So while all relationships inherently have some bias, a strong argument can be made that Lasley et al. (2016) has the least bias of commonly used relationships and was therefore adopted for use herein.

Figure 3 shows the proposed r_d relationship for M 5.5 and M 7.5, along with the r_d values predicted by a few commonly used relationships. The Liao and Whitman (1986) relationship is solely a function of depth and was adopted for use in the Youd et al. (2001) liquefaction evaluation procedures, which are widely used in practice. Cetin (2000) proposed r_d relationships that were adopted for use in the Cetin et al. (2004), Moss et al. (2006), and Kayen et al. (2013) simplified liquefaction evaluation procedures. Finally, as mentioned previously, the Idriss (1999) r_d relationship was adopted for use in the Idriss and Boulanger (2008) and Boulanger and Idriss (2014) liquefaction evaluation procedures. As shown in Figure 3a, the Lasley et al. (2016) r_d relationship yields lower values than all the other relationship for smaller magnitude events. Additionally, the Lasley et al. (2016) relationship yields lower values than all the other relationships, except for the Cetin (2000) relationship, for larger magnitude events (Figure 3b).

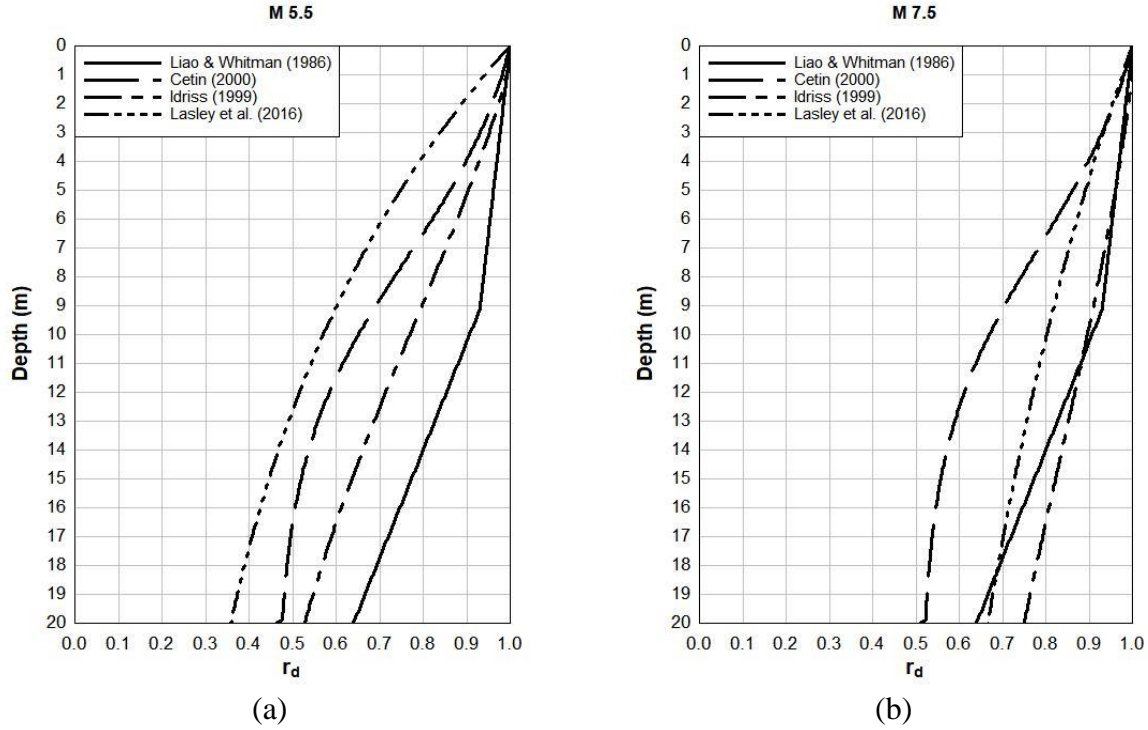


Fig. 3 Comparison of commonly used r_d relationships proposed by Liao and Whitman (1986), Cetin (2000), Idriss (2000), and Lasley et al. (2016) (Eq. 2) for two different earthquake scenarios: (a) M 5.5 and $a_{max} = 0.1g$, and (b) M 7.5 and $a_{max} = 0.3g$. Note: Liao and Whitman (1986) relationship is only a function of depth; Idriss (1999) and Lasley et al. (2016) (Eq. 2) are only dependent on M and depth; and Cetin (2000) is dependent on M , a_{max} , and depth.

3.2 Magnitude Scaling Factor: MSF

Development of a MSF relationship that overcomes all the shortcomings listed above for the Idriss and Boulanger (2008) and Boulanger and Idriss (2014) relationships is not as straightforward as developing the new r_d relationships. The reason for this is that there are many more issues with existing MSFs than there are with the r_d relationships. As a result, a new approach needed to be used to compute MSFs, as opposed to implementing an existing approach using a more comprehensive dataset and a more rigorous regression analysis.

Converting an erratic/random loading to an “equivalently damaging” sinusoidal loading having a given amplitude, frequency, and number of cycles is central to macro-level metal fatigue theories

(e.g., Green and Terri 2005; Hancock and Bommer 2005). For soil liquefaction, the soil's resistance to liquefaction is independent of the frequency of loading, for a large range of frequencies (e.g., Riemer et al. 1994) and for historical reasons the amplitude of the equivalently damaging sinusoidal loading is set equal to the 0.65 times the maximum value of the erratic/random loading (e.g., Whitman 1971; Seed and Idriss 1971). Accordingly, only the number of equivalent cycles, n_{eq} , needs to be determined. The Seed et al. (1975) procedure for computing n_{eq} underlies many of the shortcomings of the Idriss and Boulanger (2008) and Boulanger and Idriss (2014) MSF relationships listed previously.

In lieu of using the Seed et al. (1975) procedure for computing n_{eq} , the approach proposed by Green and Terri (2005) was selected for the Groningen project. This approach is an alternative implementation of the P-M fatigue theory that better accounts for the nonlinear behaviour of the soil than the Seed et al. (1975) variant. In this approach, dissipated energy is explicitly used as the damage metric. n_{eq} is determined by equating the energy dissipated in a soil element subjected to an earthquake motion to the energy dissipated in the same soil element subjected to a sinusoidal motion of a given amplitude and a “duration” of n_{eq} . Dissipated energy was selected as the damage metric because it has been shown to correlate with excess pore pressure generation in saturated cohesionless soil samples subjected to undrained cyclic loading (e.g., Green et al. 2000; Polito et al. 2008). Furthermore, from a microscopic perspective, the energy is thought to be predominantly dissipated by the friction between sand grains as they move relative to each other as the soil skeleton breaks down, which is requisite for liquefaction triggering.

Conceptually, the Green and Terri (2005) approach for computing n_{eq} is shown in Figure 4. Stress and strain time-histories at various depths in the soil profile are obtained from a site response analysis. By integrating the variation of shear stress over shear strain, the cumulative dissipated energy per unit volume of soil can be computed (i.e., the cumulative area bounded by the shear stress-shear strain hysteresis loops). n_{eq} is then determined by dividing the cumulative dissipated energy for the entire earthquake motion by the energy dissipated in one equivalent cycle. For historical reasons, the shear stress amplitude of the equivalent cycle (τ_{avg}) is taken as $0.65 \cdot \tau_{max}$ (where τ_{max} is the maximum induced cyclic shear stress, τ_c , at a given depth), and the dissipated energy associated with the equivalent cycle is determined from the constitutive model used in the

294 site response analysis.

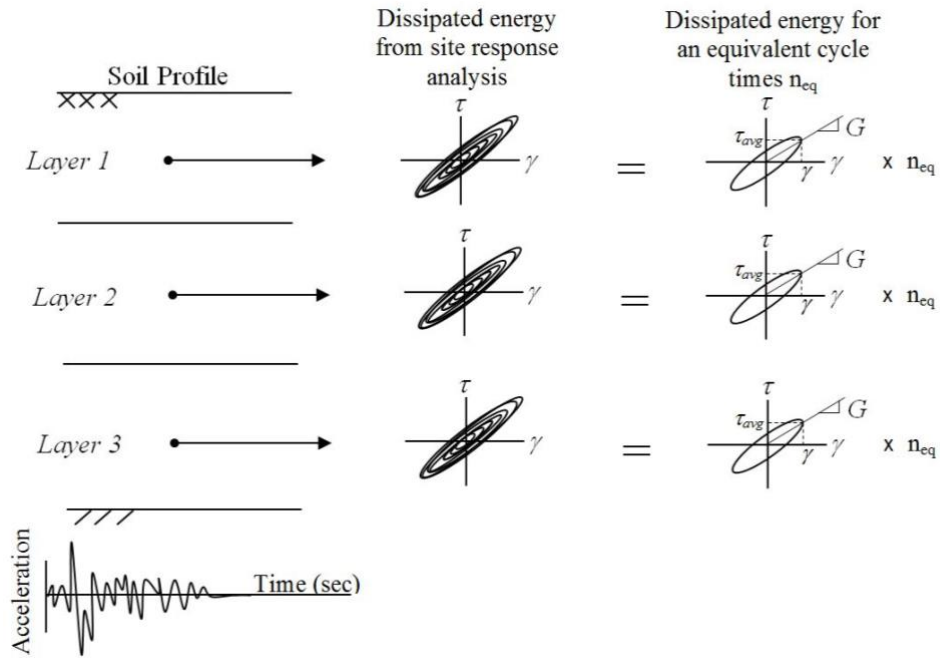


Fig. 4 Illustration of the proposed procedure to compute n_{eq} . In this procedure, the energy dissipated in a layer of soil, as computed from a site response analysis, is equated to the energy dissipated in an equivalent cycle of loading multiplied by n_{eq} .

As noted above, one of the shortcomings of the Seed et al. (1975) variant of the P-M fatigue theory is the way in which multi-directional shaking is taken into account. Specifically, each of the two horizontal components of ground motion is treated separately, inherently assuming that both components have similar characteristics. However, analysis of recorded motions has shown this is not always the case, particularly in the near fault region (e.g., Green et al. 2008; Carter et al. 2016). In contrast, Green and Terri (2005) accounted for multi-directional shaking by performing separate site response analyses for each horizontal component in a pair of motions, adding the energy dissipated at the respective depths for each component of motion, and setting the amplitude of the equivalent cycle as 0.65 times the geometric mean of the maximum shear stresses experienced at a given depth. This approach is referred to as “Approach 2” in Lasely et al. (2017) and is used herein because it better accounts for differences in the characteristics in the two horizontal components of motion.

Lasley et al. (2017) implemented the Green and Terri (2005) approach for computing n_{eq} using the same motions and profiles used by Lasley et al. (2016) to develop their r_d relationship. Their proposed n_{eq} relationship is:

$$\ln(n_{eq}) = 0.4605 - 0.4082 \cdot \ln\left(\frac{a_{max}}{g}\right) + 0.2332 \cdot M + \varepsilon_{Total} \quad (3a)$$

where a_{max} is in units of g and ε_{Total} is a zero-mean, normally distributed random variable with standard deviation σ_{Total} given by:

$$\sigma_{Total}(z) = \max\left[0.5399 - \frac{z}{26.4}(0.5399 - 0.4626), 0.4626\right] \quad (3b)$$

where z is depth in meters. The dependency of n_{eq} on a_{max} in Eq. (3a) was chosen because of the observed negative correlation of strong ground-motion duration with a_{max} (e.g., Bradley 2011; Bommer et al. 2016). Also, the functional form of this correlation is not an impediment to implementation because the simplified liquefaction evaluation procedures require both the magnitude (for MSFs and r_d) and a_{max} as input variables.

The b value that is needed to relate n_{eq} to MSFs (e.g., Figure 2) can also be determined from the constitutive model used in the site response analysis, by assuming that the CSR vs. N_{liq} curve shown in Figure 2 is a contour of constant dissipated energy (Figure 5). In Figure 5, the dissipated energy for a M 7.5 earthquake, $\Delta W_{M7.5}$, is computed using:

$$\Delta W_{M7.5} = \frac{2\pi \cdot D_\gamma \cdot \tau_c^2}{G_{max} \cdot \left(\frac{G}{G_{max}}\right)_\gamma} \cdot n_{eq \ M7.5} \quad (4)$$

where D_γ is the damping ratio for the induced shear strain γ , τ_c is the cyclic shear stress, and G is the secant shear modulus. This equation is based on the assumption that the soil can be modelled as a visco-elastic material, consistent with the assumption inherent to the equivalent linear site

response algorithm. For liquefaction evaluations, τ_c used to compute $\Delta W_{M7.5}$ can be determined from the $CRR_{M7.5}$ curve from the simplified liquefaction evaluation procedure (e.g., Boulanger and Idriss 2014). Accordingly, the computed CSR vs. N_{liq} curve corresponds to a soil having a given q_{c1Ncs} and confined at an initial effective overburden stress (σ'_{vo}) (i.e., $\tau_c = CRR_{M7.5} \times \sigma'_{vo}$); the small strain shear modulus (G_{max}) for the soil should be consistent with the penetration resistance used to determine $CRR_{M7.5}$. The damping (D_γ) and the degraded secant shear modulus, $G_{max} \cdot (G/G_{max})_\gamma$, values in Eq. (4) are commensurate with the induced shear strain (γ) in the soil and can be determined iteratively from the shear modulus and damping degradation curves used to model the soil response (e.g., Darendeli and Stokoe 2001). Once the value of $\Delta W_{M7.5}$ is determined, a contour of constant dissipated energy can be computed for different amplitudes of loading by simply computing the number of cycles for the assumed loading amplitude required for the dissipated energy to equal $\Delta W_{M7.5}$. The parameter b is assumed equal to the negative of the slope of the contour of constant dissipated energy. The assumption that the CSR vs. N_{liq} curve is a contour of constant dissipated energy inherently implies that the energy dissipated in a given element of soil at the point of liquefaction triggering is unique and independent of the imposed loading characteristics. Several studies have shown that this is a reasonable assumption (e.g., Kokusho and Kaneko 2014; Polito et al. 2013).

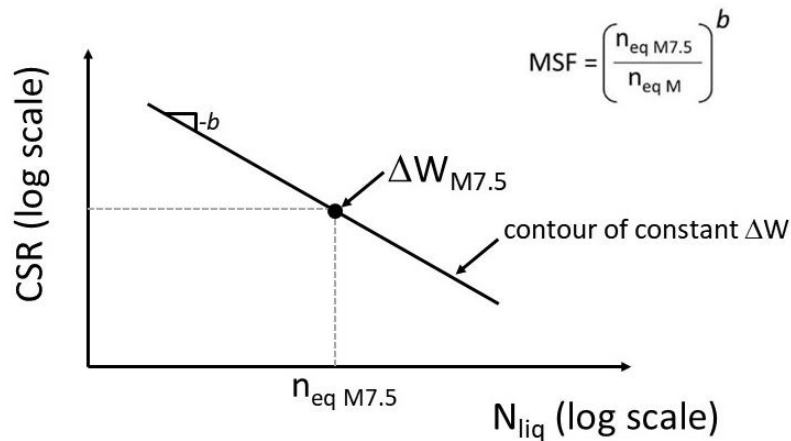


Fig. 5 A CSR vs. N_{liq} curve can be computed from shear modulus and damping degradation curves assuming the curve is a contour of constant dissipated energy. $\Delta W_{M7.5}$ can be computed using Eq. (4) and the remaining portions of the curve can be computed for different amplitudes of loading by simply computing the number of cycles for the assumed loading amplitude required for the

dissipated energy to equal $\Delta W_{M7.5}$.

The degradation curves proposed Darendeli and Stokoe (2001) were used in this study to determine the b values following the procedure illustrated in Figure 5 for a range of effective confining stresses and soil densities, with the resulting values ranging from 0.33 to 0.35. However, $b = 0.34$ for the vast majority of the confining stress-density combinations considered and was thus used herein to compute MSFs from n_{eq} . Additionally, $b = 0.34$ is consistent with laboratory curves developed from high-quality undisturbed samples obtained by freezing (Yoshimi et al. 1984). Accordingly, MSFs are computed as:

$$MSF = \left(\frac{n_{eq\ M7.5}}{n_{eq\ M}} \right)^b = \left(\frac{14}{n_{eq\ M}} \right)^{0.34} \leq 2.02 \quad (5a)$$

$$\sigma_{\ln(MSF)} = b \cdot \sigma_{\ln(n_{eq\ M})} = 0.34 \cdot \sigma_{\ln(n_{eq\ M})} \quad (5b)$$

where $\sigma_{\ln(MSF)}$ is a first order approximation for the standard deviation of the natural log of the MSF, $n_{eq\ M}$ and $n_{eq\ M7.5}$ are computed using Eq. (3a), and $\sigma_{\ln(n_{eq\ M})}$ is computed using Eq. (3b).

To compute $n_{eq\ M7.5}$ using Eq. (3a), M is set to 7.5 and a corresponding value for a_{max} needs to be assumed (i.e., $a_{max7.5}$). The value of $a_{max7.5}$ was determined by computing the average a_{max} for the case histories in the Boulanger and Idriss (2014) SPT and CPT liquefaction case history databases ranging in magnitude from M 7.4 to M 7.6. The average a_{max} for the 116 case histories that fell within this magnitude range was ~ 0.35 g. Using this value for $a_{max7.5}$, $n_{eq\ M7.5}$ was computed to be ~ 14 . This value is similar to that determined by Seed et al. (1975), i.e., $n_{eq\ M7.5} = 15$. However, the value reported by Seed et al. (1975) represents the average for two horizontal components of motion, while the value computed herein represents the combined influence of both components of motion (Approach 2, Lasley et al. 2017). As a result, the value computed herein is approximately half of that computed by Seed et al. (1975). This difference is attributed to both the significantly larger ground motion database used by Lasley et al. (2017) to develop Eq. (3), where the motions used by Lasley et al. (2017) represented a broader range of magnitudes and site-to-source distances compared to those used by Seed et al. (1975), and to the differences in the approaches used to compute n_{eq} . However, both of these differences also influence the denominator in Eq. (5a), which

minimizes their influence on the resulting MSF. The upper limit on the MSF (i.e., 2.02) corresponds to a scenario where the earthquake motions consist of a single shear stress pulse in one of the horizontal components of motion. A plot of Eq. (5a) is shown in Figure 6 for magnitudes ranging from M 5.0 to M 8.5 and a_{\max} ranging from 0.1 to 1.0 g.

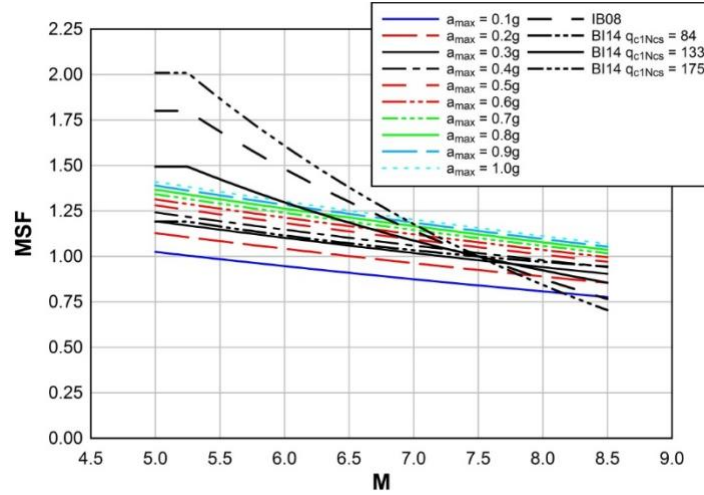


Fig. 6 For a given magnitude earthquake, MSF developed herein increases as a_{\max} increases. The reference scenario for the proposed MSF relationship (i.e., the scenario for which $MSF = 1$) is M 7.5 and $a_{\max} = 0.35$ g. Also, for comparison, the MSFs proposed by Idriss and Boulanger (2008) (IB08) and Boulanger and Idriss (2014) (BI14) are also shown.

As can be surmised from Figure 6, for a given magnitude event, the further a site is from the source, in general, the lower the a_{\max} , the longer the duration of the motion, and hence, the lower the MSF. This negative correlation between a_{\max} and ground motion duration for motions for a given event is most pronounced in the near fault region, where forward directivity results in higher amplitude, shorter duration motions and reverse directivity results in lower amplitude, longer duration motions (e.g., Somerville et al. 1997). However, this negative correlation is not limited to the near fault region but, rather, is operative across the entire area that is subjected to shaking (e.g., Bradley 2011; Bommer et al. 2016).

Figure 6 also shows a comparison of the MSF developed herein with those proposed by Idriss and Boulanger (2008) and Boulanger and Idriss (2014), where the latter is shown for $q_{c1Ncs} = 84, 133$, and 175 atm. As may be observed from this figure, for a given value of a_{\max} the MSF developed

herein has about the same dependency on magnitude as the MSF proposed by Boulanger and Idriss (2014) for $q_{c1Ncs} = 84$ atm (i.e., medium dense sand), as indicated by similar slopes of the MSF curves. However, the difference between the two is that the former is a function of a_{max} , with MSF for a given magnitude increasing as a_{max} increases.

Finally, it is emphasized that the influence of the MSF presented in Figure 6 on the predicted CSR^* should not be viewed in isolation. For example, the proposed MSF have lower values for smaller magnitude events, relative to Idriss and Boulanger (2008) relationship, and therefore will result in a higher predicted CSR^* . However, this trend will be offset, more or less, for smaller magnitude events by the reduction in r_d per the Lasley et al. (2016) relationship (Figure 3). Accordingly, any assessments in the trends in the changes to CSR^* need to consider both the use of both the Lasley et al. (2016) r_d relationship and the newly proposed MSF, which were consistently developed.

3.3 “Unbiased” $CRR_{M7.5}$ curve

The Lasley et al. (2016) r_d relationship and the MSF relationship developed herein were used to reanalyse the CPT liquefaction case history database compiled by Boulanger and Idriss (2014); all other parameters/relationships used to analyse the case history data were the same as those used by Boulanger and Idriss (2014). These case histories were then used to regress a new “unbiased” deterministic liquefaction triggering curve (i.e., $CRR_{M7.5}$ curve), which is shown in Figure 7 and given by:

$$CRR_{M7.5} = \exp \left\{ \left(\frac{q_{c1Ncs}}{113} \right) + \left(\frac{q_{c1Ncs}}{1000} \right)^2 - \left(\frac{q_{c1Ncs}}{140} \right)^3 + \left(\frac{q_{c1Ncs}}{137} \right)^4 - 2.8119 \right\} \leq 0.6 \quad (6)$$

where q_{c1Ncs} is computed using the procedure outlined in Boulanger and Idriss (2014). This curve approximately corresponds to a probability of liquefaction $[P(liq)]$ of 35% (total uncertainty) and to the Boulanger and Idriss (2014) $P(liq) = 15\%$ (model uncertainty) $CRR_{M7.5}$ curve; note that Boulanger and Idriss (2014) only state their $CRR_{M7.5}$ curves in terms of model uncertainty, not total uncertainty.

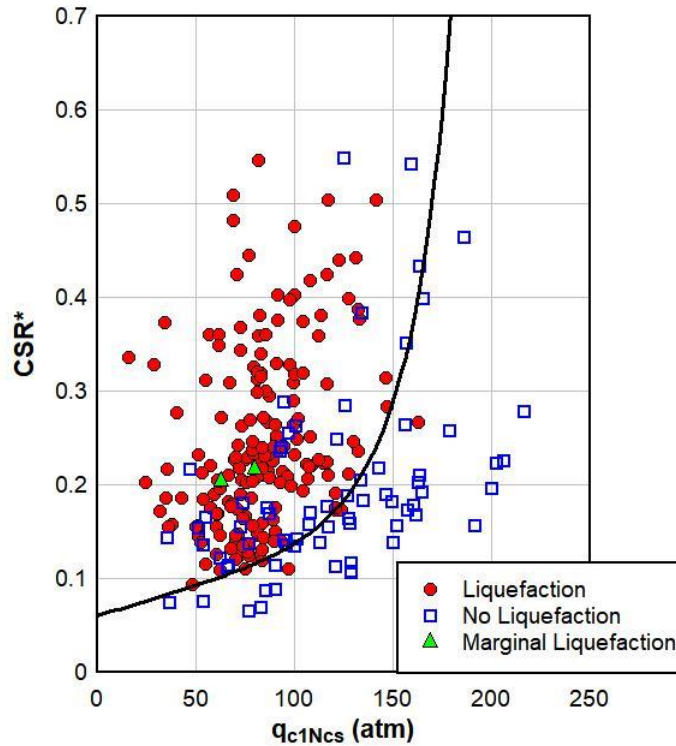


Fig. 7 “Unbiased” deterministic CRR_{M7.5} curve regressed from liquefaction case history data from Boulanger and Idriss (2014) that were reanalysed using Lasley et al. (2016) r_d relationship and MSF developed herein.

4 Assessment of liquefaction hazard in Groningen

To determine whether a Groningen-wide liquefaction hazard assessment is warranted, a liquefaction hazard pilot study is being performed first, wherein the study area was selected to simultaneously satisfy three criteria: (a) proximity to the region of highest shaking hazard; (b) sampling of areas with sand deposits that are thick, shallow, young, and loose; and (c) sampling of multiple site-response zones used in developing the Groningen-specific ground-motion model (Rodriguez-Marek et al. 2017). The location of the pilot study area is shown in Figure 8, along with the cumulative thicknesses of the Holocene sand deposits that comprise the Naaldwijk formation which is considered to have the highest liquefaction potential in the region (Korff et al. 2017). However, before the liquefaction pilot study can be performed, Groningen-specific r_d and MSF relationships must be developed.

The Groningen-specific r_d and MSF relationships will be used in conjunction with the “unbiased” $CRR_{M7.5}$ curve shown in Figure 7 and given by Eq. (6) to assess the liquefaction hazard of the pilot study area. The basis for using the $CRR_{M7.5}$ curve shown in Figure 7 without adjustment is because the capacity of the soil to resist liquefaction is an inherent property of the soil and is not dependent on the characteristics of the seismic demand. The influence of any bias that exists in the “unbiased” $CRR_{M7.5}$ curve resulting from inherent bias in the Lasley et al. (2016) r_d relationship and the newly proposed MSF will be minimized if the Groningen-specific relationships are developed following the same approaches that were used by Lasley et al. (2016, 2017) and presented above.

The soil/geologic profiles and ground motions used to develop the Groningen-specific relationships are detailed below.

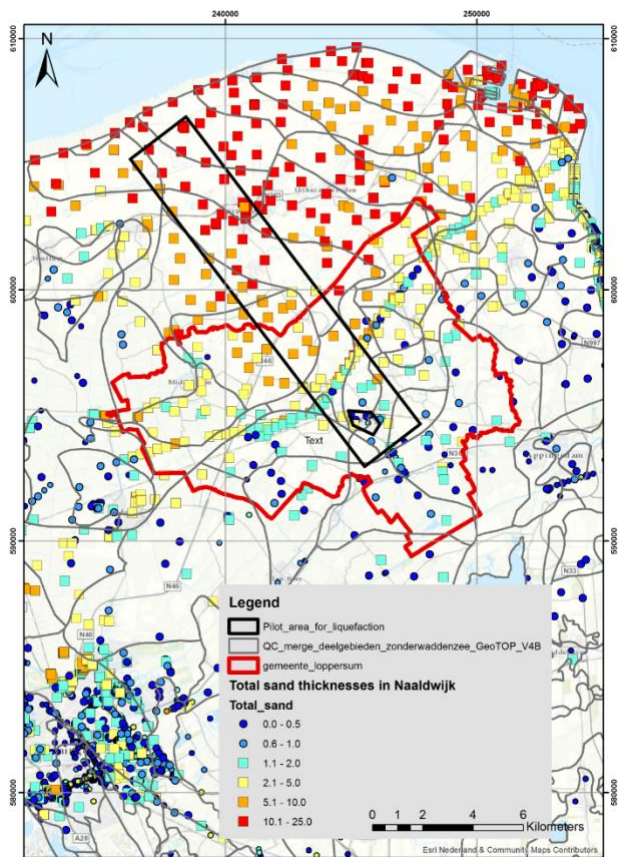


Fig. 8 Location of the liquefaction pilot study area across the Groningen gas field. Also shown are the cumulative thicknesses (m) of the Holocene sand deposits that comprise the Naaldwijk formation.

4.1 Groningen-specific r_d and MSF relationships

The geological setting of Groningen, including detailed cross sections, is described in Kruiver et al. (2017a), and the velocity model from the selected reference rock horizon (at ~ 800 m depth) to the ground surface is described in detail by Kruiver et al. (2017b). An example of the resulting V_s profiles is shown in Figure 9. The unit weights of the strata in the profiles are also needed for the site response analyses. Towards this end, the assignment of unit weight is based on representative values for stratigraphic lithological units derived from CPTs using Lunne et al. (1997). For some of the deeper formations, the density is assumed to be constant, consistent with the borehole logs from two deep boreholes (Kruiver et al. 2017a, b).

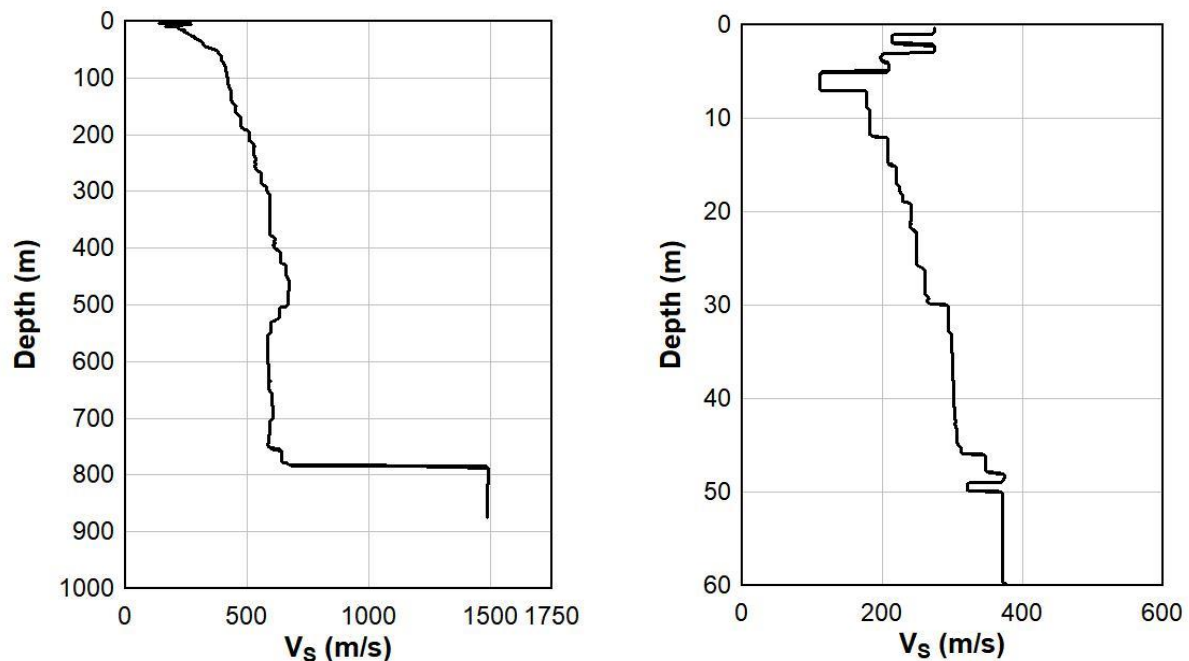


Fig. 9 Sample V_s profile at the location of one of the many ground-motion recording stations in the field. The plot on the left is the full profile down to reference rock horizon (depth of ~800 m), and the plot on the right is an enlarged view of the upper 60 m of the profile. (Rodriguez-Marek et al. 2017)

The software EXSIM (Motazedian and Atkinson 2005; Boore 2009) was used in conjunction with the Groningen-specific model parameters to generate motions at the reference horizon (Bommer et al. 2017) for magnitudes ranging from M 3.5 to M 7.0 and epicentral distances ranging from 0.1

to 60 km. The lower bound was chosen on the basis of no liquefaction having been observed in the field to date and to explore the full range of potential triggering events, despite the fact that globally there is no reliable evidence of liquefaction triggering by earthquakes smaller than M 4.5 (Green and Bommer 2018). The upper value in the maximum magnitude distribution is M 7.25 as determined by an expert panel (Bommer and van Elk 2017).

Once developed, the Groningen-specific r_d and MSF relationships can be used in conjunction with the $CRR_{M7.5}$ curve shown in Figure 7 to compute the FS_{liq} at depth in profiles in Groningen subjected to induced earthquake motions. The computation of liquefaction hazard curves that will be used to determine whether the hazard due to liquefaction is significant enough to require the consequences from liquefaction to be assessed is discussed next.

4.2 Planned output from the liquefaction hazard study

The liquefaction hazard will be calculated using a Monte Carlo method (Bourne et al. 2015) wherein probability distributions for activity rates (Bourne and Oates 2017), event locations and magnitudes, and resulting ground motions will be sampled such that the simulated future seismic hazard is consistent with historical seismic and reservoir compaction datasets. For each event scenario, the developed Groningen-specific relationships will be used to compute the FS_{liq} as a function of depth for ~100 profiles across the pilot study area.

The “Ishihara inspired LPI” (LPI_{ish}) framework will be used to relate computed FS_{liq} to the predicted the severity of surficial liquefaction manifestation, which has been shown to correlate to liquefaction damage potential for level ground sites. The LPI_{ish} framework was proposed by Maurer et al. (2015a) and is a conceptual and mathematical merger of the Ishihara (1985) H_1 - H_2 chart and Liquefaction Potential Index (LPI) framework (Iwasaki et al. 1978). The most notable differences between the original LPI and LPI_{ish} frameworks are that the latter better accounts for the influence of the non-liquefiable crust on the severity of surficial liquefaction manifestations (Green et al. 2018) and more appropriately weights the contribution of shallower liquefied layers to surficial manifestations (van Ballegooy et al. 2014). The LPI_{ish} framework was chosen for this study because it has been shown to yield more accurate predictions of the severity of surficial

liquefaction manifestations than competing indices (Maurer et al. 2015a, b): LPI (Iwasaki et al. 1978) and LSN (van Ballegooy et al. 2014).

The output from the liquefaction pilot study will be liquefaction hazard curves for the ~100 sites in the study area, where the hazard curves show the annual frequency of exceedance (AFE) of varying LPI_{ish} values for a site. Consistent with the requirements of NPR 9998-2017 (NPR 9998 2017), which was specifically developed for the Groningen field, LPI_{ish} values corresponding to an AFE of $\sim 4 \times 10^{-4}$ (or a 2475-year return period) will be of interest. The results from this pilot study will differ from previous liquefaction studies performed for Groningen, where liquefaction was evaluated in previous studies for earthquake scenarios (i.e., ground motions and magnitudes) corresponding to a given return period (i.e., a “pseudo-probabilistic” approach).

The optimal LPI_{ish} thresholds corresponding to different severities of surficial liquefaction manifestations are dependent on the liquefaction triggering procedure used to compute FS_{liq} and the characteristics of the profile. However, without liquefaction case history data to develop Groningen-specific thresholds, the thresholds proposed by Iwasaki et al. (1978) will be conservatively (Maurer et al. 2015c) used in the pilot study with the LPI_{ish} framework (i.e., $LPI_{ish} < 5$: no to minor surficial liquefaction manifestations are predicted; $LPI_{ish} > 15$: severe surficial liquefaction manifestations are predicted).

5 Discussion and conclusions

The presence of saturated loose deposits of young sands in the Groningen field region creates the necessity to assess the potential for liquefaction triggering by the earthquakes being induced by the gas production as an integral component of the seismic risk analysis. The application of liquefaction hazard assessment procedures calibrated for larger-magnitude tectonic earthquakes in other regions has resulted in predictions of potentially catastrophic liquefaction effects, with severe implications for buildings and for infrastructure such as dikes. Despite the fact that these estimates are often associated with earthquake scenarios that are only fractionally greater than the lower bound for events that have been observed globally to trigger liquefaction (Green and Bommer

2018), the dissemination of such results has raised great concern regarding liquefaction hazard in Groningen.

Due to the unique characteristics of both the seismic hazard and the geologic profiles/soil deposits in Groningen, direct application of existing variants of the simplified liquefaction evaluation procedure is deemed inappropriate for assessing the liquefaction hazard of the region, including the Idriss and Boulanger (2008) procedure recommended in the NPR 9998-2017 and the updated variant, Boulanger and Idriss (2014). Accordingly, efforts were first focused on re-analyzing the liquefaction case histories that were compiled for natural earthquakes to remove bias in their interpretation. Towards this end, new depth-stress reduction factor (r_d) and number of equivalent cycles (n_{eq})/magnitude scaling factor (MSF) relationships for shallow crustal active tectonic regimes were developed and used in the reanalysis of the cone penetration test (CPT) “liquefaction” and “no liquefaction” case histories compiled by Boulanger and Idriss (2014). These case histories were then used to regress a new “unbiased” deterministic liquefaction triggering curve (or cyclic resistance ratio curve: $CRR_{M7.5}$). The “unbiased” procedure can be readily adapted to evaluate liquefaction potential in regions with unique profiles and/or ground motions, such as Groningen. This is being achieved by using similar approaches to those employed to develop the new r_d and MSF relationships for tectonic earthquakes (Lasley et al. 2016, 2017) to develop Groningen-specific relationships using motions and soil profiles characteristic to Groningen.

The liquefaction hazard will be calculated using a Monte Carlo method wherein probability distributions for activity rates, event locations and magnitudes, and resulting ground motions are sampled such that the simulated future seismic hazard is consistent with historical seismic and reservoir compaction datasets for events having magnitudes ranging from **M** 3.5 to **M** 7.0. For each event scenario, the Groningen-specific relationships will be used to compute the factor of safety (FS_{liq}) against liquefaction as a function of depth for ~100 profiles across the liquefaction pilot study area and corresponding Ishihara inspired Liquefaction Potential Index (LPI_{ish}) (Maurer et al. 2015a) hazard curves are being computed for each profile. The hazard curves specify the return periods of different severities of surficial liquefaction manifestations, with the severities corresponding to a return period of 2475 years being of interest per the NPR 9998-2017. This is in marked contrast to previous liquefaction hazard studies performed for Groningen that used a

pseudo-probabilistic approach, where the FS_{liq} or LPI is computed for an earthquake scenario (i.e., ground motions and magnitude) corresponding to a given return period.

The framework of the liquefaction hazard pilot study is in complete accord with the safety philosophy of the NPR 9998-2017 and is particularly well suited to the specific nature of the time-dependent induced seismicity being considered. The results of the study will form the basis on which decisions will be made regarding the need for implementing mitigation measures. The liquefaction hazard study is benefiting significantly from the broader efforts to assess the regional seismic hazard in Groningen, to include the development of a regional velocity model (Kruiver et al. 2017a, b), site response model (Rodriguez-Marek et al. 2017), and ground-motion prediction model (Bommer et al. 2017).

Acknowledgments

This research was partially funded by Nederlandse Aardolie Maatschappij B.V. (NAM) and the National Science Foundation (NSF) grants CMMI-1030564 and CMMI-1435494. This support is gratefully acknowledged. This study has also significantly benefited from enlightening discussions with colleagues at Shell, Deltares, Arup, Fugro, Beca, and on the NEN liquefaction task force. The authors also gratefully acknowledge the constructive comments by the anonymous reviewers. However, any opinions, findings, and conclusions or recommendations expressed in this material are those of the authors and do not necessarily reflect the views of the NSF or NAM.

References

Bird JF, Bommer JJ (2004) Earthquake losses due to ground failure. *Engineering Geology* 75(2):147-179.

Bommer JJ, van Elk J (2017) Comment on ‘The maximum possible and the maximum expected earthquake magnitude for production-induced earthquakes at the gas field in Groningen, the Netherlands’ by Gert Zöller and Matthias Holschneider. *Bulletin of the Seismological Society of America* 107(3):1564-1567.

Bommer JJ, Dost B, Edwards B, Stafford PJ, van Elk J, Doornhof D, Ntinalexis M (2016) Developing an Application-Specific Ground-Motion Model for Induced Seismicity. *Bulletin of the Seismological Society of America* 106(1):158–173.

Bommer JJ, Stafford PJ, Edwards B, Dost B, v. Dedem E, Rodriguez-Marek A, Kruiver P, van Elk J, Doornhof D, Ntinalexis M (2017) Framework for a ground-motion model for induced seismic hazard and risk analysis in the Groningen gas field, the Netherlands. *Earthquake Spectra* 33(2):481-498.

Boore DM (2009) Comparing stochastic point-source and finite-source ground-motion simulations: SMSIM and EXSIM. *Bulletin of the Seismological Society of America* 99:3202-3216.

Boulanger RW, Idriss IM (2014) CPT and SPT Based Liquefaction Triggering Procedures. Report No. UCD/CGM-14/01, University of California at Davis, Davis, CA.

Bourne SJ, Oates SJ (2017) Extreme threshold failures within a heterogeneous elastic thin-sheet account for the spatial-temporal development of induced seismicity within the Groningen gas field. *Journal of Geophysical Research: Solid Earth* 122. DOI: 10.1002/2017JB014356.

Bourne SJ, Oates SJ, Bommer JJ, Dost B, van Elk J, Doornhof D (2015) A Monte Carlo method for probabilistic seismic hazard assessment of induced seismicity due to conventional gas production. *Bulletin of the Seismological Society of America* 105:1721–1738.

Bradley BA (2011) Correlation of significant duration with amplitude and cumulative intensity measures and its use in ground motion selection. *Journal of Earthquake Engineering* 15:809–832.

Carter WL, Green RA, Bradley BA, Wotherspoon LM, Cubrinovski M (2016) Spatial Variation of Magnitude Scaling Factors During the 2010 Darfield and 2011 Christchurch, New Zealand, Earthquakes. *Soil Dynamics and Earthquake Engineering* 91:175-186.

Cetin KO (2000) Reliability-based assessment of seismic soil liquefaction initiation hazard. Ph.D. Thesis, University of California at Berkeley, Berkeley, CA.

Cetin KO, Seed RB, Der Kiureghian A, Tokimatsu K, Harder LF, Kayen RE, Moss RES (2004) Standard penetration test-based probabilistic and deterministic assessment of seismic soil liquefaction potential. *Journal of Geotechnical and Geoenvironmental Engineering* 130(12):1314-1340.

Darendeli MB, Stokoe II KH (2001) Development of a new family of normalized modulus reduction and material damping curves. Geotechnical Engineering Report GD01-1, University of Texas at Austin, Austin, TX.

Green RA, Bommer JJ (2018) What is the smallest earthquake magnitude that can trigger liquefaction? *Earthquake Spectra* (*in review*).

Green RA, Terri GA (2005) Number of equivalent cycles concept for liquefaction evaluations - revisited. *Journal of Geotechnical and Geoenvironmental Engineering* 131(4):477-488.

Green RA, Mitchell JK, Polito CP (2000). An energy-based excess pore pressure generation model for cohesionless soils. *Proceedings of The John Booker Memorial Symposium – Developments in Theoretical Geomechanics* (D.W. Smith and J.P. Carter, eds.), A.A. Balkema, Rotterdam, The Netherlands, 383-390.

Green RA, Lee J, White TM, Baker JW (2008) The significance of near-fault effects on liquefaction. *Proc. 14th World Conf. on Earthquake Engineering*, Paper No. S26-019.

Green RA, Cubrinovski M, Cox B, Wood C, Wotherspoon L, Bradley B, Maurer B (2014) Select liquefaction case histories from the 2010-2011 Canterbury earthquake sequence. *Earthquake Spectra* 30:131-153.

- Green RA, Maurer BW, van Ballegooy S (2018) The influence of the non-liquefied crust on the severity of surficial liquefaction manifestations: Case history from the 2016 Valentine's Day earthquake in New Zealand. Proc. Geotechnical Earthquake Engineering and Soil Dynamics V (GEESD V), Austin, TX, 10-13 June.
- Hancock J, Bommer JJ (2005) The effective number of cycles of earthquake ground motion. Earthquake Engineering and Structural Dynamics 34:637-664.
- Idriss IM (1999) An update to the Seed-Idriss simplified procedure for evaluating liquefaction potential. Proc., TRB Workshop on New Approaches to Liquefaction, Publication No. FHWA-RD-99-165, Federal Highway Administration.
- Idriss IM, Boulanger RW (2008) Soil liquefaction during earthquakes. Monograph MNO-12, Earthquake Engineering Research Institute, Oakland, CA, 261 pp.
- Ishihara K (1985) Stability of natural deposits during earthquakes. Proc. 11th Intern. Conf. on Soil Mechanics and Foundation Engineering, San Francisco, CA, USA, 1:321-376.
- Iwasaki T, Tatsuoka F, Tokida K, Yasuda S (1978) A practical method for assessing soil liquefaction potential based on case studies at various sites in Japan. Proc. 2nd Intern. Conf. on Microzonation, Nov 26-Dec 1, San Francisco, CA, USA.
- Kayen R, Moss RES, Thompson EM, Seed RB, Cetin KO, Der Kiureghian A, Tanaka Y, Tokimatsu K (2013) Shear-wave velocity-based probabilistic and deterministic assessment of seismic soil liquefaction potential. Journal of Geotechnical and Geoenvironmental Engineering 139(3):407-419.
- Kokusho T, Kaneko Y (2014) Dissipated & strain energies in undrained cyclic loading tests for liquefaction potential evaluations. Proc. Tenth US National Conf. on Earthquake Engineering, July 21-25, 2014, Anchorage, Alaska, DOI: 10.4231/D3DR2P89D

Korff M, Wiersma A, Meijers P, Kloosterman F, de Lange G, van Elk J, Doornhof D (2017) Liquefaction mapping for induced seismicity based on geological and geotechnical features. Proc. 3rd Intern. Conf. on Performance-Based Design in Earthquake Geotechnical Engineering (PBDIII), Vancouver, Canada, 16-19 July, 2017.

Kruiver PP, Wiersma A, Kloosterman FH, de Lange G, Korff M, Stafleu J, Busscher F, Harting R, Gunnink JL, Green RA, van Elk J, Doornhof D (2017a). Characterisation of the Groningen subsurface for seismic hazard and risk modelling. *Netherlands Journal of Geosciences* 96(5):s215-s233.

Kruiver PP, van Dedem E, Romijn R, de Lange G, Korff M, Stafleu J, Gunnink JL, Rodriguez-Marek A, Bommer JJ, van Elk J, Doornhof D (2017b) An integrated shear-wave velocity model for the Groningen gas field, The Netherlands, *Bulletin of Earthquake Engineering*. doi: 10.1007/s10518-017-0105-y.

Lasley S, Green RA, Rodriguez-Marek A (2014) Comparison of equivalent-linear site response analysis software. Proc. 10th National Conf. on Earthquake Engineering (10NCEE), Anchorage, AK, 21-25 July.

Lasley S, Green RA, Rodriguez-Marek A (2016). A new stress reduction coefficient relationship for liquefaction triggering analyses. Technical Note, *Journal of Geotechnical and Geoenvironmental Engineering* 142(11):06016013-1.

Lasley S, Green RA, Rodriguez-Marek A (2017) Number of equivalent stress cycles for liquefaction evaluations in active tectonic and stable continental regimes. *Journal of Geotechnical and Geoenvironmental Engineering* 143(4):04016116-1.

Liao SSC, Whitman RV (1986) Catalogue of liquefaction and non-liquefaction occurrences during earthquakes. Research Report Department of Civil Engineering, Massachusetts Institute of Technology, Cambridge, MA.

- Lunne T, Robertson PK, Powell JJM (1997) Cone Penetration Testing in Geotechnical Practice, EF Spon/Blackie Academic, Routledge Publishers, London, United Kingdom, 312 pp.
- Maurer BW, Green RA, Taylor, O-DS (2015a) Moving towards an improved index for assessing liquefaction hazard: Lessons from historical data. *Soils and Foundations* 55(4):778-787.
- Maurer BW, Green RA, Cubrinovski M, Bradley BA (2015b) Calibrating the Liquefaction Severity Number (LSN) for competing liquefaction evaluation procedures: A case study in Christchurch, New Zealand. *Proc. 6th Intern. Conf. on Earthquake Geotechnical Engineering (6ICEGE)*, Christchurch, New Zealand, 2-4 November.
- Maurer BW, Green RA, Cubrinovski M, Bradley BA (2015c) Fines-Content Effects on Liquefaction Hazard Evaluation for Infrastructure in Christchurch, New Zealand. *Soil Dynamics and Earthquake Engineering* 76:58-68.
- Motazedian D, Aktinson GM (2005) Stochastic finite-fault modelling based on a dynamic corner frequency. *Bulletin of the Seismological Society of America* 95:995-1010.
- Moss RES, Seed RB, Kayen RE, Stewart JP, Der Kiureghian A, Cetin KO (2006) CPT-based probabilistic and deterministic assessment of in situ seismic soil liquefaction potential. *Journal of Geotechnical and Geoenvironmental Engineering* 132(8):1032-1051.
- NPR 9998 (2017) Assessment of structural safety of buildings in case of erection, reconstruction and disapproval – Basis rules for seismic actions: induced earthquakes. NEN, Delft, Netherlands.
- National Research Council (NRC) (2016) State of the Art and Practice in the Assessment of Earthquake-Induced Soil Liquefaction and Consequences. Committee on Earthquake Induced Soil Liquefaction Assessment, National Research Council, The National Academies Press, Washington, DC.
- Polito CP, Green RA, Lee J (2008) Pore pressure generation models for sands and silty soils

subjected to cyclic loading. *Journal of Geotechnical and Geoenvironmental Engineering* 134(10):1490-1500.

Polito C, Green RA, Dillon E, Sohn C (2013) The effect of load shape on the relationship between dissipated energy and residual excess pore pressure generation in cyclic triaxial tests. *Canadian Geotechnical Journal* 50(9):1118-1128.

Riemer MF, Gookin WB, Bray JD, Arango I. (1994) Effects of loading frequency and control on the liquefaction behavior of clean sands. *Geotechnical Engineering Report No. UCB/GT/94-07*, Department of Civil and Environmental Engineering, University of California at Berkeley, Berkeley, CA.

Rodriguez-Marek A, Kruiver PP, Meijers P, Bommer JJ, Dost B, van Elk J, Doornhof D (2017) A regional site-response model for the Groningen gas field. *Bulletin of the Seismological Society of America* 107(5):2067-2077.

Seed HB, Idriss IM (1971) Simplified procedure for evaluating soil liquefaction potential. *Journal of the Soil Mechanics and Foundations Division* 97(SM9):1249–273.

Seed HB, Idriss IM, Makdisi F, Banerjee N (1975) Representation of irregular stress time histories by equivalent uniform stress series in liquefaction analysis. Report Number EERC 75-29, Earthquake Engineering Research Center, College of Engineering, University of California at Berkeley, Berkeley, CA.

Somerville PG, Smith NF, Graves RW, Abrahamson NA (1997) Modification of empirical strong ground motion attenuation relationships to include the amplitude and duration effects of rupture directivity. *Seismological Research Letters* 68(1):199-222.

Stafford PJ, Zurek BD, Ntinalexis M, Bommer JJ (2018) Extensions to the Groningen ground-motion model for seismic risk calculations: Component-to-component variability and spatial correlation. This volume.

Ulmer KJ, Upadhyaya S, Green RA, Rodriguez-Marek A, Stafford PJ, Bommer JJ, van Elk J
 (2018) A Critique of b-values Used for Computing Magnitude Scaling Factors. Proc. Geotechnical
 Earthquake Engineering and Soil Dynamics V (GEESD V), Austin, TX, 10-13 June.

van Ballegooy S, Malan P, Lacrosse V, Jacka ME, Cubrinovski M, Bray JD, O'Rourke TD,
 Crawford SA, Cowan H (2014) Assessment of liquefaction-induced land damage for residential
 Christchurch. Earthquake Spectra 30(1):31-55.

van Elk J, Doornhof D, Bommer JJ, Bourne SJ, Oates SJ, Pinho R, Crowley H (2017) Hazard and
 risk assessments for induced seismicity in Groningen. Netherlands Journal of Geoscience
 96(5):s259-s269.

Whitman RV (1971) Resistance of soil to liquefaction and settlement. Soils and Foundations
 11(4):59-68.

Yoshimi Y, Tokimatsu K, Kaneko O, Makiyara Y (1984). Undrained cyclic shear strength of dense
 Niigata sand. Soils and Foundations, 24(4):131-145.

Youd TL, Idriss IM, Andrus RD, Arango I, Castro G, Christian JT, Dobry R, Finn WDL, et al.
 (2001) Liquefaction Resistance of Soils: Summary Report from the 1996 NCEER and 1998
 NCEER/NSF Workshops on Evaluation of Liquefaction Resistance of Soils. Journal of
 Geotechnical and Geoenvironmental Engineering 127(4):297-313.